# $[Pb(H_2O)]^{2+}$ and $[Pb(OH)]^{+}$: Four-component density functional theory calculations, correlated scalar relativistic constrained-space orbital variation energy decompositions, and topological analysis

Christophe Gourlaouen
*Laboratoire de Chimie Théorique-UMR 7616 CNRS/UPMC, Université Pierre et Marie Curie-Paris 6, Case Courrier 137-4, place Jussieu, F. 75252 Paris Cedex 05, France*

Jean-Philip Piquemal
*Laboratory of Structural Biology, National Institute of Environmental Health Science, Mail Drop F0-08, P.O. Box 12233, Research Triangle Park, North Carolina 27709*

Olivier Parisel[a)]
*Laboratoire de Chimie Théorique-UMR 7616 CNRS/UPMC, Université Pierre et Marie Curie-Paris 6, Case Courrier 137-4, place Jussieu, F. 75252 Paris Cedex 05, France*

(Received 26 January 2006; accepted 21 February 2006; published online 4 May 2006)

Within the scope of studying the molecular implications of the $Pb^{2+}$ cation in environmental and polluting processes, this paper reports Hartree-Fock and density functional theory (B3LYP) four-component relativistic calculations using an all-electron basis set applied to $[Pb(H_2O)]^{2+}$ and $[Pb(OH)]^{+}$, two complexes expected to be found in the terrestrial atmosphere. It is shown that full-relativistic calculations validate the use of scalar relativistic approaches within the framework of density functional theory. $[Pb(H_2O)]^{2+}$ is found $C_{2v}$ at any level of calculations whereas $[Pb(OH)]^{+}$ can be found bent or linear depending of the computational methodology used. When $C_s$ is found the barrier to inversion through the $C_{\infty v}$ structure is very low, and can be overcome at high enough temperature, making the molecule floppy. In order to get a better understanding of the bonding occurring between the $Pb^{2+}$ cation and the $H_2O$ and $OH^-$ ligands, natural bond orbital and atoms-in-molecule calculations have been performed. These approaches are supplemented by a topological analysis of the electron localization function. Finally, the description of these complexes is refined using constrained-space orbital variation complexation energy decompositions. © *2006 American Institute of Physics*. [DOI: 10.1063/1.2186994]

## I. INTRODUCTION

Heavy metals or their cations are known to be involved in biological processes where they usually act as poisons.[1] The particular toxicity of lead, widely scattered in nature from centuries, is well established:[2–5] lead poisoning can involve either Pb(II) and Pb(IV) compounds, but all sources evolve, *in vivo* or in aqueous media, to a number of Pb(II) compounds responsible for saturnism.[6]

The $Pb^{2+}$ cation has a [Xe] $4f^{14}5d^{10}6s^26p^0$ electronic configuration and exhibits an especially versatile character with respect to the hard and soft acids and bases (HSAB) theory.[7,8]

Moreover, it appears to be an *intermediate acid* able to bind to a large number of biochemically relevant ligands[9] within very flexible coordination modes (monocoordinated to decacoordinated).[10,11]

Although complex, the aqueous chemistry of lead has been investigated for many years in order to develop, among others, water or soil cleanup processes, probes, sensors, or sequestering agents. Some theoretical modelings of the solvation or hydration of $Pb^{2+}$ have been reported.[12–14] At the opposite, its gas-phase chemistry is less known although a number of species have been experimentally detected.[11,15,16] Theoretical investigations on other related small and formally monoliganded plumbyl species are available; see, for example, the neutral $Pb(H_2O)$, $Pb(HO_2)$, $PbO_2$, PbOH, $PbH_2$, PbO, $PbO_2$, and $PbO_3$ species involved in atmospheric chemistry.[17–19] It should be pointed out that, within this series, only $PbH_2$ has been spectroscopically characterized by means of its infrared spectrum.[20,21]

It seems to be particularly difficult to generate the monohydrate $[Pb(H_2O)]^{2+}$ in the gas phase. It has been suggested that this might be due to the redox reaction involving $Pb^{2+}$ and $H_2O$ where an effective charge-transfer occurs, leading to $Pb^+$ and $H_2O^+$ species. A repulsive Coulombian explosion might then happen. In fact, this complex has been very recently produced and identified by means of time-of-flight mass spectrometry[16] and has been found to be stable from theoretical computations.[12] Nevertheless, to the best of our knowledge, no spectroscopic data (rotational or vibrational spectra) are available for that complex, nor for $[Pb(OH)]^{+}$.

Theoretical investigations of such compounds require addressing two different problems. The first one is the well-known role of electronic correlation effects on complexation energies and geometries. The second one arises from the fact

[a)]Author to whom correspondence should be address. Fax: 003 314 427 4117. Electronic mail: parisel@lct.jussieu.fr

 

that relativistic effects in $Pb^{2+}$ could be strong enough to significantly modify the expected physicochemical properties of its complexes.[22–29]

Up to now, it has been possible to treat both problems, correlation and relativity, all together, by using scalar relativistic pseudopotentials coupled to the correlated techniques usually used in quantum chemistry.[9,12,13,17,18,30–38] However, to the best of our knowledge, no four-component correlated relativistic all-electron calculations have been performed on $[Pb(H_2O)]^{2+}$, nor on $[Pb(OH)]^{+}$, although the examination of relativistic effects has been reported at various levels of theory for PbO,[32] $PbCl_4$,[32] $Pb_2$,[39] $PbH_4$,[32,40] and $Pb(CH_3)_3H$.[40]

In this contribution, we report such calculations and compare them to pseudopotential scalar relativistic computations (Secs. III and IV). This way, it should be possible to distinguish between the respective roles of correlation and relativity as well as to comfort the relevancy of using pseudopotential within density functional theory (DFT) scalar one-component relativistic calculations, an approach that could easily be applicable to large size systems (Sec. V).

We also provide (Sec. VI) some insights about the nature, covalent or electrostatic, of the bonding between $Pb^{2+}$ and $H_2O$ or $OH^-$ by means of natural bond orbital[41–43] (NBO) analysis, and atoms-in-molecules[44] (AIM) or topological analysis[45,46] of the electron localization function[47–49] (ELF) which is a refined complement to the previous ones. Finally, an analysis of the complexation energies is provided within the constrained-space orbital variation[50,51] (CSOV) framework, the results of which might also be used to parametrize polarizable molecular mechanics, in order, for example, to investigate biomimetic or bioinspired metalloprotein models relevant to lead poisoning.

## II. COMPUTATIONAL DETAILS

### A. Generals

The scalar calculations have been performed using the GAUSSIAN03 package[52] within the restricted Hartree-Fock (RHF) and B3LYP[53,54] formalisms. This functional, which was successfully used in a previous work devoted to hydrates of heavy cations,[55] was chosen as it has proven to provide geometries and energies close to CCSD(T) for species closely related to those investigated here.[17–19] The standard 6-31+G** basis set was used to describe the O and H atoms, whereas scalar relativistic pseudopotentials[56] (PPs) were used for $Pb^{2+}$. These are either the LANL2DZ PP by Hay and Wadt[57] coupled to a double-zeta quality basis set, or the large-core relativistic SDD pseudopotentials by Kuelche *et al.*[58] For the sake of comparison with other high-quality pseudopotentials, we also have investigated the averaged relativistic effective PPs (AREPs)[59] known in the EMSL database[60] under the CRENBS ("small core": valence $=5d,6s,6p$) and CRENBS ("large core": valence$=6s,6p$) acronyms. The valence basis sets associated with these PPs, which have been optimized on neutral atoms for LANL2DZ, CRENBL, and CRENBS, and on *quasineutral* atoms for SDD, are used as such and are characterized by the following contraction patterns. For LANL2DZ, the valence electrons correspond to $6s^2$ and are described using a $(3s3p)/[2s2p]$ contraction. For the SDD pseudopotential, the same valence definition is retained and a $(4s4p1d)/[2s2p1d]$ contraction is used. The CRENBS pseudopotential considered here is coupled to a valence $(3s3p)/[1s1p]$ Gaussian basis set. In the following, we will use the CRENBLD acronym to refer to the CRENBL pseudopotential provided by EMSL and relying on a totally uncontracted basis set, $(3s3p4d)/[3s3p4d]$. CRENBLC will be used to refer to the original CRENBL pseudopotential relying on the $[1s1p1d]$ contraction.[59]

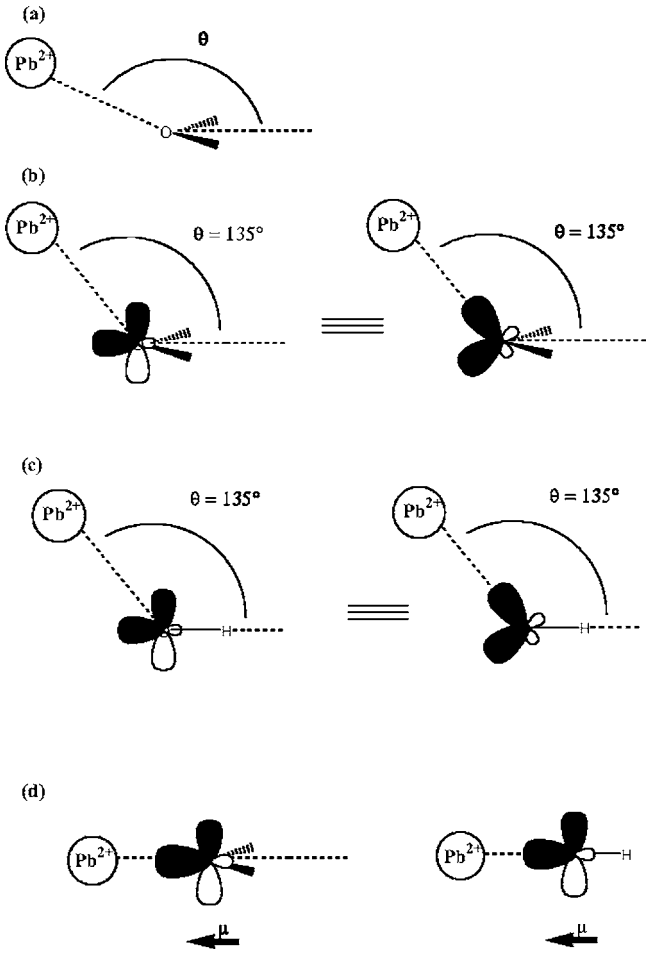


FIG. 1. (a) Definition of the dihedral angle Θ characterizing the out-of-plane wagging deformation in the $[Pb(H_2O)]^{2+}$ complex. This angle corresponds to the angle between the Pb–O axis and the bisecting axis of the HOH valence angle. [(b) and (c)] Most favorable approaches of the cation toward the water molecule or the $OH^-$ anion. (b) *Orbital Control*: most efficient overlap ($\Theta=135°$); (d) *electrostatic control*: most efficient interaction between the cation charge and the water molecule static dipole ($\Theta=180°$).

The all-electron (AE) calculations have been performed using Faegri's basis sets on the heavy atom; such basis are known to be of at least double-zeta quality.[61]

The four-component calculations have been performed using the DIRAC code[62] which has been recently extended to the DFT formalism.[63,64] The Dirac-Coulomb Hamiltonians,[65] (thereafter, DHF/AE: Dirac-HF, DB3LYP/AE: Dirac-B3LYP) have been retained. The uncontracted small component basis sets were generated from the large component sets according to the kinetic balance condition. Finite size Gaussian nuclei were used and the nuclear exponents were taken

TABLE I. Geometrical parameters (Å and degrees) and complexation energies (kcal/mol) for the $[Pb(H_2O)]^{2+}$ complex.

| | Pseudopotential approach | | | | | | | | All-electron approach | | | |
|---|---|---|---|---|---|---|---|---|---|---|---|---|
| | LANL2DZ | | CRENBLD CRENBLC | | CRENBS | | SDD | | Nonrelativistic | | Relativistic | |
| | RHF | B3LYP | RHF | B3LYP | RHF | B3LYP | RHF | B3LYP | RHF | B3LYP | DHF | DB3LYP |
| $r$(Pb–O) | 2.271 | 2.257 | 2.443 | 2.445 | 2.390 | 2.368 | 2.364 | 2.339 | 2.343 | 2.342 | 2.347 | 2.338 |
| | | | 2.445 | 2.435 | | | | | | | | |
| $r$(OH) | 0.961 | 0.983 | 0.958 | 0.979 | 0.959 | 0.980 | 0.959 | 0.981 | 0.961 | 0.981 | 0.960 | 0.982 |
| | | | 0.958 | 0.979 | | | | | | | | |
| $b$(HOH) | 127.0 | 126.9 | 126.9 | 127.1 | 127.0 | 126.8 | 126.9 | 126.7 | 126.9 | 126.8 | 127.0 | 126.6 |
| | | | 127.1 | 127.2 | | | | | | | | |
| Θ | 180.0 | 180.0 | 180.0 | 180.0 | 180.0 | 180.0 | 180.0 | 180.0 | 180.0 | 180.0 | 180.0 | 180.0 |
| | | | 180.0 | 180.0 | | | | | | | | |
| $\Delta E$ | −61.2 | −67.4 | −50.3 | −53.4 | −53.9 | −59.7 | −55.0 | −61.2 | −53.4 | −59.0 | −53.5 | −61.0 |
| | | | −51.9 | −56.7 | | | | | | | | |
| $D_0$ | 54.7 | 60.1 | 44.8 | 49.0 | 49.0 | 53.8 | 49.2 | 54.6 | | | | |
| | | | 46.4 | 49.7 | | | | | | | | |

from a list of values recommended by Visscher and Dyall.[66] All (SS/SS)- and (SS/LL)-type integrals have been explicitly retained in the calculations.

### B. Optimizations and vibrational analysis

Full geometry optimizations have been performed, always starting from a $C_s$ structure [see Fig. 1(a)] allowed to relax either to the $C_{2v}$ symmetry characterized by a ($Pb^{2+}OHH$) dihedral angle Θ (wagging out of plane) equal to 180.0° in $[Pb(H_2O)]^{2+}$ or to $C_{\infty v}$ for $[Pb(OH)]^{+}$.

The nature of the stationary points encountered has been characterized by a vibrational analysis performed within the harmonic approximation. No scaling procedure has been applied. The vibrational frequencies have been used as such to evaluate $\delta E_{ZPE}$, the zero-point- energy (ZPE) correction. The normal modes will thereafter be labeled as follows for $[Pb(H_2O)]^{2+}$: $\omega$ for the wagging out-of-plane mode, $\beta$ for the (HOH) bending mode, $\rho$ for the Pb–O stretching mode, $\kappa$ for the rocking mode, and $\sigma_-$ and $\sigma_+$ for, respectively, the antisymmetric and symmetric stretching modes of the OH bonds. For $[Pb(OH)]^{+}$, the notations become $\rho$ for the Pb–O stretching mode, $\beta$ for the (PbOH) bending mode, and $\sigma$ for the OH stretching mode. However, it should be kept in mind that couplings may occur that complicate the description of the normal modes in terms of chemically relevant internal coordinates. The anharmonic corrections to the vibrational wave numbers have been determined following the perturbation procedure implemented in GAUSSIAN03 according to the formalism developed by Barone.[67,68]

### C. Interaction energies

The complexation energies used hereafter are defined according to

$$\Delta E = E(\text{complex}) - E(\text{cation}) - E(\text{Ligand}).$$

The basis set superposition error (BSSE) to $\Delta E$ has been determined according to the counterpoise procedure.[69,70]

The bonding energy, positive, is defined as

$$D_0 = -[\Delta E + \delta E_{BSSE} + \delta E_{ZPE}],$$

where

$$\delta E_{ZPE} = \text{ZPE(complex)} - \text{ZPE(Ligand)}.$$

## III. THE $[Pb(H_2O)]^{2+}$ COMPLEX

### A. Structure and bonding

As seen from Table I, a $C_{2v}$ structure [Fig. 1(d)] is obtained whatever the level of calculation considered. Using a different basis set for O and H (DZP,[71] no diffuse functions on oxygen) and a different pseudopotential for Pb (SBKJC[72]), $r$(Pb–O) bond lengths ranging from 2.28 (B3LYP) to 2.31 (CC-D) Å have been reported, depending on the level of calculation.[12] The reference DB3LYP/AE calculations gives a Pb–O distance of 2.34 Å.

The DB3LYP/AE value of 2.34 Å is thus in fair agreement with that obtained from scalar coupled cluster calculations. This bond length is, as expected, much shorter than the one computed in the neutral $[Pb(H_2O)]$ complex (2.74 Å for both the $^1A''$ and $^3A''$ states):[18] here, both electrostatic and covalence effects (donation from the water lone pairs to the

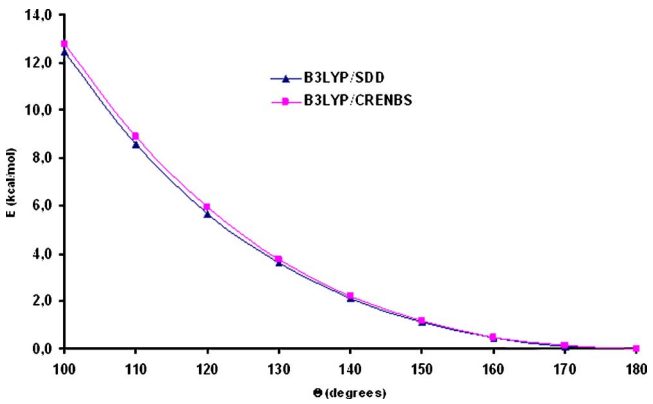


FIG. 2. Wagging potential energy curve as a function of Θ (see text for definition), for the $[Pb(H_2O)]^{2+}$ complex.

TABLE II. B3LYP vibrational frequencies ($cm^{-1}$) of the $[Pb(H_2O)]^{2+}$ and $[Pb(OH)]^{+}$ complexes. The parenthesized values correspond to harmonic vibrational frequencies corrected for anharmonicity (see text for details).

| | LANL2DZ | CRENBLD | CRENBLC | CRENBS | SDD |
|---|---|---|---|---|---|
| | | | $[Pb(H_2O)]^{2+}$ | | |
| $\rho$ | 359 | 336 | 342 | 341 (335) | 343 (335) |
| $\omega$ | 523 | 486 | 507 | 491 (528) | 484 (512) |
| $\beta$ | 656 | 607 | 630 | 639 (638) | 641 (638) |
| $\kappa$ | 1669 | 1666 | 1675 | 1669(1633) | 1664(1629) |
| $\sigma_+$ | 3605 | 3655 | 3653 | 3635(3457) | 3627(3448) |
| $\sigma_-$ | 3676 | 3729 | 3726 | 3712(3512) | 3703(3502) |
| | | | $[Pb(OH)]^{+}$ | | |
| $\rho$ | 244 | 342 | 416 | 422 (289) | 87 |
| $\beta$ | 648 | 596 | 594 | 604 (590) | 623 |
| $\sigma$ | 3880 | 3848 | 3829 | 3821(3637) | 3883 |

$6p$ vacant orbitals of the cation) shorten this distance. Amazingly, this bond length is quite insensitive to the inclusion of relativity or correlation. The same remark applies for the bending angle (HOH).

The inclusion of electronic correlation effects (RHF/AE versus B3LYP/AE: −0.001 Å) as well as the inclusion of relativistic effects (RHF/AE versus DHF/AE: +0.004 Å) leave the Pb–O bond length almost unchanged.

The B3LYP/SDD geometry is in almost perfect agreement with the DB3LYP/AE results, as is the B3LYP/CRENBS Pb–O bond length. In contrast, B3LYP/CRENBLD gives a too long bond length (by more than 0.1 Å) whereas B3LYP/LANL2DZ gives a too short one, by more than 0.08 Å.

It is worth noting that the wagging mode may have a large amplitude: as seen from Fig. 2, the out-of-plane deformation angle evolves in the (150°–210°) range with energy variations less than 1 kcal/mol with respect to the $C_{2v}$ minimum. It follows that the harmonic approximation used to evaluate the corresponding out-of-plane vibration may not be reliable.

At the B3LYP/SDD level, the harmonic vibration wave numbers amount to (Table II, $cm^{-1}$) 343($\rho$), 484($\omega$), 641($\beta$), 1664($\kappa$), 3627($\sigma_+$), and 3703($\sigma_-$).

When taking the anharmonic corrections into account, these values become 335($\rho$), 512($\omega$), 638($\beta$), 1629($\kappa$), 3448($\sigma_+$), and 3502($\sigma_-$).

At the B3LYP/CRENBS level, the harmonic vibrational wave numbers are: 341($\rho$), 491($\omega$), 639($\beta$), 1669($\kappa$), 3635($\sigma_+$), and 3712($\sigma_-$); and the anharmonic: 335($\rho$), 528($\omega$), 638($\beta$), 1633($\kappa$), 3457($\sigma_+$), and 3512($\sigma_-$).

Clearly, the anharmonic corrections are similar for both the SDD and CRENBS pseudopotentials. A decrease by about 200 $cm^{-1}$ for the two OH stretching modes is observed in both cases: such an anharmonicity, about 5.5% of the harmonic value, is commonly observed for such modes. The $\kappa$ mode decreases by only 30 $cm^{-1}$, and the $\rho$ and $\beta$ modes remain almost unchanged and are thus harmonic. More inter-

TABLE III. Geometrical parameters (Å and degrees) and complexation energies (kcal/mol) for the $[Pb(OH)]^{+}$ complex. $[HPbO]^{+}$ is found linear with $r(PbO)=1.915$ Å and $r(HPb)=1.818$ Å; it lies 121.8 kcal/mol above $[Pb(OH)]^{+}$. The associated vibrational frequencies are ($cm^{-1}$) 252 (bending), 696 (Pb–O stretching), and 1559 (Pb–H stretching).

| | Pseudopotential approach | | | | | | | | All-electron approach | | | |
|---|---|---|---|---|---|---|---|---|---|---|---|---|
| | LANL2DZ | | CRENBLD CRENBLC | | CRENBS | | SDD | | Nonrelativistic | | Relativistic | |
| | RHF | B3LYP | RHF | B3LYP | RHF | B3LYP[a] | RHF | B3LYP | RHF | B3LYP | DHF | DB3LYP |
| $r$(Pb−O) | 1.869 | 1.895 | 2.083<br>2.086 | 2.125<br>2.134 | 2.007 | 2.036 | 1.949 | 1.957 | 1.968 | 1.998 | 1.975 | 2.013 |
| $r$(OH) | 0.944 | 0.966 | 0.948<br>0.948 | 0.968<br>0.970 | 0.948 | 0.970 | 0.945 | 0.966 | 0.943 | 0.966 | 0.948 | 0.971 |
| $b$(PbOH) | 180.0 | 180.0 | 135.0<br>136.9 | 143.3<br>140.5 | 141.2 | 139.6 | 161.4 | 180.0 | 162.4 | 162.9 | 143.7 | 141.0 |
| $\Delta E$ | −374.0 | −382.8 | −343.4<br>−343.1 | −343.7<br>−348.8 | −352.1 | −363.6 | −358.2 | −368.8 | −364.3 | −369.4 | −359.1 | −370.6 |
| $D_0$ | 366.7 | 374.8 | 340.1<br>337.4 | 341.1<br>341.6 | 347.3 | 358.1 | 352.6 | 362.5 | | | | |

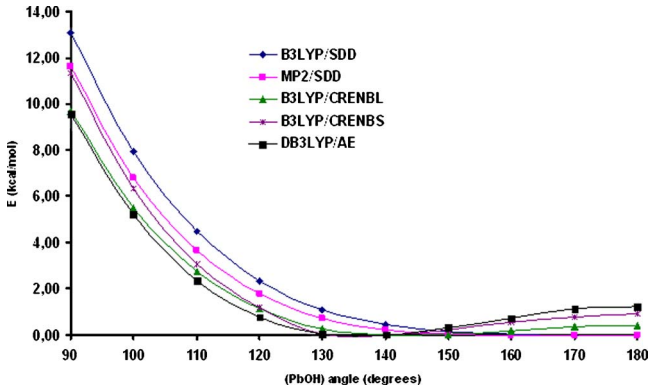


FIG. 3. Potential energy curves for the $[Pb(OH)]^{+}$ complex as a function of the (PbOH) bending angle.

esting is the increase by about 40 $cm^{-1}$ for the wagging out-of-plane $\omega$ mode: this shift amounts to about 7.5% of the harmonic value. As anticipated, the wagging mode appears anharmonic.

### B. Binding energy

The computed DB3LYP/AE reference value for the complexation energy amounts to $\Delta E=-61.0$ kcal/mol. Values ranging from −64.1 (HF) to −73.5 (B3LYP) kcal/mol have been reported for scalar relativistic calculations.[12] Both B3LYP/CRENBLD and B3LYP/LANL2DZ calculations provide complexation energies differing by more than 5 kcal/mol from the DB3LYP/AE value.

Because of the computational cost required to estimate the ZPE correction at the DB3LYP/AE level, it has been estimated at the B3LYP/SDD level (Table II). This leads to $D_0=+54\pm1$ kcal/mol for this complex if restricting to the *a priori* most reliable B3LYP/CRENBS and B3LYP/SDD calculations.

## IV. THE $[Pb(OH)]^{+}$ COMPLEX

### A. Structure

Table III gathers most of the geometry optimization results.

At the B3LYP/CRENBS level of calculation, the $[HPbO]^{+}$ structure lies 121.8 kcal/mol above $[Pb(OH)]^{+}$: this connectivity will thus not be investigated further in this paper. The discussion will hereafter focus on $[Pb(OH)]^{+}$ and, first, on the geometry: linear or bent.

If correlation is neglected, all approaches but HF/LANL2DZ predict a bent structure. However, if we follow the conclusions of the previous section, the LANL2DZ pseudopotential should not be considered as reliable for this kind of plumbyl complexes.

At correlated levels, still all but B3LYP/SDD calculations predict a bent structure [Fig. 1(c)]. For the DB3LYP/AE approach, the bending PbOH angle amounts to 141° and the complexation energy to −370.6 kcal/mol. Such a bent structure seems to be confirmed by the B3LYP/CRENBS calculation (139.6°). Such angular values are close to that expected if the interaction is under orbital control [Fig. 1(c)]. Surprisingly, the B3LYP/SDD calculation (180.0°) does not agree with the DB3LYP/AE computation. We have performed an optimization constrained to linearity at the DB3LYP/AE level: the complexation energy has been found to be −369.8 kcal/mol. At this level, there is thus less than 1 kcal/mol between the linear and the bent structure. The potential energy curves relative to the bending mode are reported in Fig. 3 for several computational approaches. It is clear that, whatever the methodology used, these curves are especially flat which explains why the bending angle found from different levels of calculations can vary from 139.6° to 180.0°: from Fig. 3, it is seen that the bending can scan an amplitude of 60° (from about 120° to about 180°) with energy variations not exceeding 1.5 kcal/mol.

Such a large amplitude, which might be twice as large if no barrier exists, leads to question the validity of the harmonic approximation in evaluating vibrational frequencies.

The calculations have been complemented (Table IV) by MP2/SDD and CCSDT/CRENBS computations which give $b(PbOH)=160.6°$ and 138.9°, respectively. For all methods giving a bent minimum, optimizations constrained to linearity give transition states, the imaginary frequencies of which correspond to the bending mode (Table V). B3LYP/CRENBS thus appears to be the best approach to reproduce the geometrical parameters given by the DB3LYP/AE calculations. At this level, the purely electronic energy barrier between the optimized 139.6° structure and the 180° transition state amounts to 0.9 kcal/mol. Including the ZPE corrections reduces this value by 186 $cm^{-1}$ and gives a barrier height of about 0.4 kcal/mol.

TABLE IV. Geometrical parameters (Å and degrees), complexation energies (kcal/mol), and vibrational frequencies ($cm^{-1}$) for the $[Pb(OH)]^{+}$ complex at the MP2 and CCSD(T) levels of calculation.

| | CCSD(T) | | |
|---|---|---|---|
| | CRENBS | SDD | MP2 SDD |
| $r$(Pb−O) | 2.044 | 1.991 | 1.980 |
| $r$(OH) | 0.969 | 0.966 | 0.967 |
| $b$(PbOH) | 138.9 | 153.1 | 160.6 |
| $\Delta E$ | −353.3 | −362.1 | −360.2 |
| $D_0$ | 346.9 | 354.7 | 353.0 |
| $\rho$ | 462 | 34 | 128 |
| $\beta$ | 605 | 613 | 623 |
| $\rho$ | 3880 | 3912 | 3908 |

TABLE V. Geometrical parameters (Å and degrees), complexation energies (kcal/mol), and vibrational frequencies ($cm^{-1}$) for the $[Pb(OH)]^{+}$ complex constrained to linearity.

| | B3LYP CRENBLD | B3LYP CRENBLC | B3LYP CRENBS | DB3LYP AE |
|---|---|---|---|---|
| $r$(Pb−O) | 2.104 | 2.109 | 2.010 | 1.989 |
| $r$(OH) | 0.966 | 0.968 | 0.968 | 0.969 |
| $b$(PbOH) | 180.0 | 180.0 | 180.0 | 180.0 |
| $\Delta E$ | −343.3 | −347.9 | −362.7 | −369.8 |
| $\rho$ | 612 | 607 | 618 | |
| $\beta$ | 247$i$ | 312$i$ | 311$i$ | |
| $\sigma$ | 3872 | 3861 | 3867 | |

TABLE VI. Orbital (spinor) absolute energies (a.u.) for the water molecule $3a_1$ and $1b_1$ lone pairs, for the $OH^-$ anion $1\pi$ and $3\sigma$ lone pairs, together with the $6s^2$ and $6p^0$ levels of the $Pb^{2+}$ cation. Conventions have been chosen for the water molecule in order that the pure $2p_O$ lone pair belongs to the $B_1$ irreducible representation of the $C_{2v}$ group.

| | Pseudopotential approach | | | | | | | | All-electron approach | | | |
|---|---|---|---|---|---|---|---|---|---|---|---|---|
| | CRENBS | | CRENBLD CRENBLC | | LANL2DZ | | SDD | | Nonrelativistic | | Relativistic | |
| | RHF | B3LYP | RHF | B3LYP | RHF | B3LYP | RHF | B3LYP | RHF | B3LYP | RHF | DB3LYP |
| $H_2O\ (3a_1)^2$ | −0.581 | −0.394 | −0.581 | −0.394 | −0.581 | −0.394 | −0.581 | −0.394 | −0.581 | −0.391 | −0.581 | −0.391 |
| $H_2O\ (1b_1)^2$ | −0.510 | −0.321 | −0.510 | −0.321 | −0.510 | −0.321 | −0.510 | −0.321 | −0.510 | −0.318 | −0.510 | −0.317 |
| $OH^-\ (1\pi)^4$ | −0.104 | 0.047 | −0.104 | 0.047 | −0.104 | 0.047 | −0.104 | 0.047 | −0.104 | 0.051 | −0.104 | 0.051 |
| $OH^-\ (3\sigma)^2$ | −0.250 | −0.089 | −0.250 | −0.089 | −0.250 | −0.089 | −0.250 | −0.089 | −0.250 | −0.087 | −0.250 | −0.087 |
| $Pb^{2+}\ (6s_{1/2})^2$ | −1.118 | −1.041 | −1.105 | −1.005 | −1.112 | −1.036 | −1.101 | −1.206 | −0.967 | −0.910 | −1.109 | −1.039 |
| | | | −1.119 | −1.039 | | | | | | | | |
| $Pb^{2+}\ (6p_{1/2})^0$ | −0.494 | −0.606 | −0.479 | −0.583 | −0.493 | −0.618 | −0.483 | −0.600 | −0.472 | −0.602 | −0.522 | −0.668 |
| | | | −0.495 | −0.597 | | | | | | | −0.480[a] | −0.615[a] |
| $Pb^{2+}\ (6p_{3/2})^0$ | −0.494 | −0.606 | −0.479 | −0.583 | −0.493 | −0.618 | −0.483 | −0.600 | −0.472 | −0.602 | −0.459 | −0.588 |
| | | | −0.495 | −0.597 | | | | | | | −0.480[a] | −0.615[a] |

[a]Averaged energy between the $6p_{1/2}$ and $6p_{3/2}$ spinors.

If we now focus on the Pb–O bond length, we observe that the B3LYP/LANL2DZ value is significantly too short when compared to the DB3LYP/AE value, whereas the B3LYP/CRENBLD length is significantly too long. At variance, both CRENBS and SDD provide a bond length in good agreement with that obtained from the fully relativistic computation. Correlation slightly increases the Pb–O bond length (RHF/AE versus B3LYP/AE: −0.03 Å) as also do relativistic effects (RHF/AE versus DHF/AE: −0.04 Å).

For $[Pb(OH)]^+$ in its optimized bent structure, we have, at the B3LYP/CRENBS level, the following vibrational wave numbers ($cm^{-1}$):

harmonic: $422(\rho), 604(\beta), 3821(\sigma)$,

anharmonic: $289(\rho), 590(\beta), 3637(\sigma)$.

Once again an about 200 $cm^{-1}$ decrease of the OH stretching mode is observed. More surprisingly the anharmonic effects affect the $\rho$ mode the most: a decrease of 133 $cm^{-1}$ is observed (−31.5%!) while the bending mode $\beta$ decreases only by 2.3%. Such a behavior is rather striking: the $\beta$ mode was expected to be the least harmonic one since it exhibits the largest amplitude motion.

The situation might, however, be drastically different if, due to temperature, the barrier (0.4 kcal/mol) at $b(Pb-O-H)=180°$ could be crossed over: in such situations, the system should be considered as floppy and may exhibit a different IR signature. Such cases, the treatment of which requires a dynamic treatment, are currently under investigation and will be published in due time.

### B. Binding energy

The $\Delta E=-370.6$ kcal/mol complexation energy obtained at the DB3LYP/AE level is well reproduced by the B3LYP/SDD computation, and fairly well at the B3LYP/CRENBS level. The absolute differences amount to 1.80 and 7 kcal/mol, respectively, which correspond to relative errors of 0.5% and 1.9%. The situation is surprisingly bad for B3LYP/CRENBLD: the error amounts to 26.9 kcal/mol (7.3%). For B3LYP/LANL2DZ, the complexation energy is overestimated by 12.2 kcal/mol (3.4%), but we recall that within this approach the Pb–O length has been found significantly too short. Clearly, it is to be concluded that LANL2DZ and CRENBLD are not reliable, as such, to deal with this compound. The $D_0$ values amount to 362.5 and 358.1 kcal/mol at the B3LYP/SDD and B3LYP/CRENBS, respectively.

## V. DISCUSSION: RELIABILITY OF THE PSEUDOPOTENTIAL APPROACH

As detailed in the previous sections (Tables I and III), there is a very nice agreement between the four-component DB3LYP/AE calculations and the B3LYP/PP approach if using the SDD or CRENBS pseudopotentials. These agreements are found for the complexation energies and for the geometries, especially for the Pb–O bond length. The LANL2DZ and CRENBLD pseudopotentials perform badly, very certainly for different reasons which we will investigate in the following.

### A. The location of the 6*s* and 6*p* spinors

Table VI collects the absolute energy of the highest valence $6s_{1/2}$, $6p_{1/2}$, and $6p_{3/2}$ spinors of $Pb^{2+}$ computed using either pseudopotentials or the AE basis set.

There is a good agreement between the energies found for $6s_{1/2}$ by the B3LYP/PP approaches when compared to that computed from DB3LYP/AE on the one hand, and between the RHF/PP and DHF/AE values on the other hand. This result is in perfect agreement with the way the CREN, LANL2DZ, and SDD pseudopotentials have been elaborated (calibration on DHF calculations). The lowering of this level due to relativity is about −0.142 a.u. (DHF/AE versus RHF/AE values) but is somehow counterbalanced by a correlation energy value of 0.057 a.u. (B3LYP/AE versus RHF/AE). The energetic decrease due to coupled correlation/

relativity effects amounts to 0.072 a.u. (DB3LYP/AE versus RHF/AE) which is very close to the 0.0850 a.u. value obtained by just summing the above-mentioned correlation and relativity contributions.

For the $6p$ level, we use as a reference the DB3LYP/AE values averaged over the two $6p_{1/2}$ and $6p_{3/2}$ spinors: −0.615 a.u. The B3LYP/CRENBS (−0.606 a.u.), B3LYP/LANL2DZ (−0.618 a.u.), and B3LYP/SDD (−0.600 a.u.) compare favorably with the DB3LYP/AE value. This is clearly not the case for B3LYP/CRENBLD: this value amounts to −0.583 a.u., which, however, compares favorably to the −0.588 a.u. reported for the sole $6p_{3/2}$ spinor at the DB3LYP/AE level. The fact that the B3LYP/CRENBLD $6p$ level is too high in energy might explain the poor $\Delta E$ values obtained using this pseudopotential for both $[Pb(H_2O)]^{2+}$ and $[Pb(OH)]^{+}$. The nonprecise reproduction of the DB3LYP/AE computations by the B3LYP/LANL2DZ approach (also see the previous sections) certainly relies on the small expansion of the Gaussian basis set associated with this pseudopotential.

For the $6p_{1/2}$ spinor, the lowering due to relativity (DHF/AE versus RHF/AE) amounts to −0.05 a.u., and that due to correlation (B3LYP/AE versus RHF/AE) to −0.130 a.u. Both give a total lowering of −0.135 a.u., to be compared to the exact coupled relativity/correlation effects (DB3LYP/AE versus RHF/AE) of −0.196 a.u. For the $6p_{3/2}$ spinor, we get, respectively, +0.013 and −0.13 a.u., which results in −0.117 a.u., a value which is to be compared to the exact decrease of −0.116 a.u. obtained from a direct calculation. We thus observe a slightly more pronounced additivity of relativistic and correlation effects for $6p_{3/2}$ than for $6p_{1/2}$.

### B. Correlation versus relativity within the AE and PP approaches: Methodology

The respective role of correlation and relativity and an estimate of nonadditivity effects can be obtained from a very simple energy decomposition.[55] It relies on the following expressions where the $\Delta E$ (DB3LYP/AE) value, considered as the reference, is built from independent relativistic and correlation contributions to be added to the well-defined RHF/AE level of approximation:

$$\Delta E(\text{DB3LYP/AE}) = E_0 + E_{\text{rc}}^{\text{ex}},$$

$$E_0 = \Delta E(\text{RHF/AE}),$$

$$E_{\text{rc}}^{\text{ex}} = E_c + E_r + E_{\text{rc}}^{\text{na}}.$$

$E_{\text{rc}}^{\text{ex}}$ is the exact contribution including relativity and correlation effects. $E_c$ is the contribution issued from "pure correlation," and $E_r$ is that associated with "pure relativity." $E_{\text{rc}}^{\text{na}}$ is a nonadditive relativity/correlation crossed term.

We here have used the following decomposition to estimate pure correlation and pure relativity contributions:

$$E_c = \Delta E(\text{B3LYP/AE}) - E_0,$$

$$E_r = \Delta E(\text{DHF/AD}) - E_0.$$

The nonadditive term can therefore be expressed as

$$E_{\text{rc}}^{\text{na}} = +[\Delta E(\text{DB3LYP/AE}) - \Delta E(\text{B3LYP/AE}) - \Delta E(\text{DHF/AE}) + \Delta E(\text{RHF/AE})].$$

As relativistic effects are intrinsically included in PP calculations, only a correlation contribution can be defined within such approaches,

$$\Delta E(\text{B3LYP/PP}) = E_0 + E_c,$$

$$E_0 = \Delta E(\text{RHF/PP}),$$

$$E_c = \Delta E(\text{B3LYP/PP}) - E_0.$$

Of course, comparing these values to the $E_c$ values recovered from AE calculations is not relevant. Since the relativity effect is included in the $E_0$ value when using PPs, we thus have to compare $E_0$/PP to $(E_0+E_r)$/AE. We then have to compare $E_c$/PP with the remaining components of $\Delta E$(AE), namely, $(E_c+E_{\text{rc}}^{\text{na}})$/AE.

TABLE VII. Energy decompositions (kcal/mol): Correlation vs relativity and nonadditive component.

| | $[Pb(H_2O)]^{2+}$ | $[Pb(OH)]^{+}$ |
|---|---|---|
| | AE calculations | |
| $E_0$ | −53.4 | −364.3 |
| $E_c$ | −5.6 | −5.1 |
| $E_\tau$ | −0.1 | +5.2 |
| $E_{\text{rc}}^{\text{ex}}$ | −7.6 | −6.3 |
| $E_{\text{rc}}^{\text{na}}$ | −1.9 | −6.4 |
| $E_{\text{rc}}^{\text{na}}/\Delta E$ | 3.1% | 1.8% |
| $E_0+E_r$ | −53.5 | −359.1 |
| $E_c+E_{\text{rc}}^{\text{na}}$ | −7.5 | −11.5 |
| | $E_c$ from PP calculations | |
| SDD | −6.2 | −10.6 |
| CRENBS | −5.8 | −11.5 |
| CRENBLD | −3.1 | −0.3 |
| CRENBLC | −4.8 | −5.7 |

### C. Correlation versus relativity within the AE and PP approaches: Results

Table VII reports the energy decompositions ("relativity versus correlation") performed on $[Pb(H_2O)]^{2+}$ and $[Pb(OH)]^{+}$ for the SDD, CRENBS, and CRENBLD pseudopotentials.

The values of $E_0$/PP compare very favorably to those given by $(E_0+E_r)$/AE for SDD and CRENBS, especially for $[Pb(OH)]^{+}$, which shows that these two scalar relativistic pseudopotentials are trustworthy to account for relativity effects. The values of $E_c$/PP are also in good agreement with $(E_c+E_{\text{rc}}^{\text{na}})$/AE for SDD and CRENBS. CRENBLD exhibits, however, more pronounced deviations for both complexes and both quantities; moreover the very low value of $E_c$/CRENBLD for $[Pb(OH)]^{+}$ is especially striking and may result from the too highly located $6p$ level (cf. *supra*).

At the B3LYP/CRENBS level of calculation, and for $[Pb(H_2O)]^{2+}$, the nonadditive correlation/relativity contribution to $\Delta E$ amounts to 1.9 kcal/mol and accounts for 3.1% of the total complexation energy. This is very low when com-

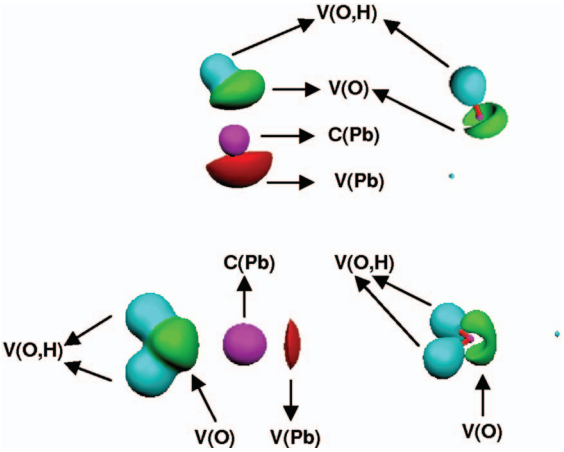


FIG. 4. (Color) ELF localization domains of $[Pb(OH)]^+$ (top) and of $[Pb(H_2O)]^{2+}$ (bottom) for $\eta$=0.45 (left) and $\eta$=0.85 (right).

pared to other monohydrate complexes: 12.5% for $[Hg(H_2O)]^{2+}$, 20.6% for $[Au(H_2O)]^+$, but remains close to the 5.7% found for $[Ag(H_2O)]^+$.[55] For $[Pb(OH)]^+$, these nonadditive effects are still lower (1.8%). Such low values of the nonadditive terms have to be connected to the quasiadditivity of relativistic and correlation effects reported previously when dealing with the location of the 6*s* and 6*p* levels. These results thus provide another hint about the quality of the SDD and CRENBS pseudopotentials, and a clue about the reliability of their transferability from atomic to molecular systems.

These two complexes are thus examples of heavy metal complexes in which, at least for the complexation energy, there is a quasiadditivity of correlation and relativity effects. This might be of interest if higher-level calculations are required: the correlation contribution could be evaluated using the state-of-the-art scalar techniques of quantum chemistry, separately from the relativistic contribution.

## VI. ON THE NATURE OF THE Pb–O BONDING: A TOPOLOGICAL ANALYSIS COMPLEMENTED BY AN ENERGY DECOMPOSITION

In order to get more insight as to the nature of the bonding in these complexes, complementary computations have been carried out: (i) charge and topological analysis and (ii) interaction energy decomposition.

### A. Computational procedures: NBO, AIM, and ELF

First, NBO[41] analyses have been performed on both complexes. Such calculations have been supplemented by AIM[44] calculations, which has provided another set of charges. Finally, the ELF[47,48] has been used to get a refined point of view [Fig. 4]: the topological analysis of this function and the integration over the localization basins have been realized.[45,46] The NBO calculations have been done according to the implementation made in GAUSSIAN 03,[52] and the AIM and ELF computations follow those implemented in the TOPMOD package.[73,74] The results have been collected in Tables VIII and IX and are issued from B3LYP electron densities.

For the sake of comprehension, it is recalled that the NBO analysis relies on an *optimal* transformation (which will not be detailed here) of the *canonical delocalized* wave

TABLE VIII. "Atomic" populations ($e^-$) and charges ($e^+$) from B3LYP calculations. NNA refers to "nonnuclear attractor."

| | $[Pb(H_2O)]^{2+}$ | | | | $[Pb(OH)]^+$ | | | |
|---|---|---|---|---|---|---|---|---|
| | Pb | O | H H | NNA | Pb | O | H | NNA |
| | | | | SDD | | | | |
| Populations | | | | | | | | |
| NBO | 2.07 | 9.14 | 0.78 | 0.00 | 2.29 | 9.29 | 0.41 | 0.00 |
| AIM | 0.09 | 9.81 | 0.46 | 1.62 | 0.08 | 9.78 | 0.25 | 1.86 |
| Charges | | | | | | | | |
| NBO | 1.93 | −1.14 | 1.22 | 0.00 | 1.71 | −1.29 | 0.59 | 0.00 |
| AIM | 3.91 | −1.81 | 1.54 | −1.64 | 3.92 | −1.78 | 0.75 | −1.89 |
| | | | | CRENBS | | | | |
| Populations | | | | | | | | |
| NBO | 2.07 | 9.13 | 0.78 | 0.00 | 2.33 | 9.23 | 0.43 | 0.00 |
| AIM | 0.10 | 9.76 | 0.46 | 1.64 | 0.10 | 9.76 | 0.27 | 1.83 |
| Charges | | | | | | | | |
| NBO | 1.93 | −1.13 | 1.22 | 0.00 | 1.67 | −1.23 | 0.57 | 0.00 |
| AIM | 3.90 | −1.76 | 1.54 | −1.68 | 3.90 | −1.76 | 0.73 | −1.87 |
| | | | | CRENBLC | | | | |
| Populations | | | | | | | | |
| NBO | 12.05 | 9.13 | 0.80 | 0.00 | 12.30 | 9.25 | 0.44 | 0.00 |
| AIM | 12.11 | 9.38 | 0.48 | 0.00 | 12.44 | 9.23 | 0.28 | 0.00 |
| Charges | | | | | | | | |
| NBO | 1.95 | −1.13 | 1.20 | 0.00 | 1.70 | −1.25 | 0.56 | 0.00 |
| AIM | 1.89 | −1.38 | 1.52 | 0.00 | 1.56 | −1.23 | 0.72 | 0.00 |

TABLE IX. Populations integrated over the ELF basins.

| | $[Pb(H_2O)]^{2+}$ | $[Pb(OH)]^{+}$ |
|---|---|---|
| | SDD | |
| | Six ELF basins | Four ELF basins |
| $C(O)$ | 2.12 | 2.12 |
| $V(O)$ | 2.22 | 5.75 |
| $V(O)$ | 2.10 | ··· |
| $V(H_1,O)$ | 1.70 | 1.75 |
| $V(H_2,O)$ | 1.70 | ··· |
| $V(Pb)$ | 2.14 | 2.36 |
| Charge on Pb | 1.86 | 1.64 |
| | CRENBS | |
| | Six ELF basins | Four ELF basins |
| $C(O)$ | 2.12 | 2.13 |
| $V(O)$ | 2.23 | 5.67 |
| $V(O)$ | 2.10 | ··· |
| $V(H_1,O)$ | 1.70 | 1.75 |
| $V(H_2,O)$ | 1.70 | ··· |
| $V(Pb)$ | 2.13 | 2.45 |
| Charge on Pb | 1.87 | 1.55 |
| | CRENBLC | |
| | Seven ELF basins | Five ELF basins |
| $C(O)$ | 2.12 | 2.12 |
| $V(H_1,O)$ | 1.70 | 1.72 |
| $V(H_2,O)$ | 1.70 | ··· |
| $V(O,Pb)$ | 2.24 | 5.74 |
| $V(O,Pb)$ | 2.12 | ··· |
| $C(Pb)$ | 9.93 | 9.94 |
| $V(Pb)$ | 2.17 | 2.45 |
| Charge on Pb | 1.89 | 1.56 |

function into a *localized* function in which chemists can identify one-center (core electrons and lone pairs) and two-center (bonds) contributions and, thus, interpret the molecular computations in terms of Lewis structures.

### B. Qualitative interpretation: AIM results

From Table VIII, it is immediately seen that non-nuclear attractors[75] (NNAs) appear if using AIM/SDD or AIM/CRENBS. Such critical points are rarely encountered and it is not clearly known what physical meaning is to be ascribed to them.[76] In the present case, it seems, however, clear that most part of the electrons assigned to the corresponding basins should, in fact, be related to the Pb atom. The difficulty of using AIM with large-core pseudopotentials is known for many years.[77–81] Slight modifications to such pseudopotentials have been proposed and proven to remedy such artifacts.[78,80,81] An example of such an artificial behavior is thus clearly provided here as, when turning to a small-core pseudopotential (CRENBLC), the AIM charges and populations recover a clearly significant chemical sense and the NNAs disappear (Table VIII).

### C. Qualitative interpretation: ELF results

In order to provide a refined and complementary view to the AIM results, ELF calculations have been performed. Within the framework of the topological analysis of the ELF function, space is partitioned into basins of attractors, each of them having a chemical meaning.[74] Such basins are classified as (i) core basins surrounding nuclei and (ii) valence basins, which are characterized by their synaptic order.

A core basin, $C(X)$, where $X$ stands for a nucleus, is usually representative of electrons not involved in the chemical bonding, namely, nonvalence and internal-shell electrons. The valence basins are distinguished according to the number of core basins with which they share a common boundary (synaptic order). A valence basin $V(X)$ is monosynaptic and corresponds to lone-pair or nonbonding regions. A $V(X,Y)$ basin is disynaptic: it binds the core of two nuclei $X$ and $Y$ and, thus, corresponds to a bonding region between $X$ and $Y$. In principle, the topological analysis of ELF should be restrained to all-electron densities since, without core electrons, there is no core basins and, thus, no way of rigorously define the synaptic orders of the valence basins. It has been shown, however, that it is possible to extend the ELF approach and carry out calculations using pseudopotentials.[82] If using large-core pseudopotentials, the number and the location of the valence basins are identical to the all-electron case; using small-core pseudopotentials provides an external core: well-defined basins can thus be constructed.[83]

As seen from Table IX, there is almost no difference between the ELF/SDD and ELF/CRENBS approaches. In both cases, six basins are detected for $[Pb(H_2O)]^{2+}$ and four for $[Pb(OH)]^{+}$. No disynaptic valence basins $V(Pb,O)$ are identified: this is due to the use of large-core pseudopotentials. This has some advantage in the present case as it is possible to define ELF charges for the Pb nucleus. The situation is different for ELF/CRENBLC. Indeed, as a $C(Pb)$ basin now exists (corresponding to the $5d^{10}$ electrons), two disynaptic $V(Pb,O)$ basins appear.

### D. Quantitative comparisons

#### 1. $[Pb(H_2O)]^{2+}$

At the B3LYP/SDD level of calculation, the NBO analysis (Table VIII) finds Pb(II) to have the $6s^{1.99}6p^{0.08}$ electronic configuration; that of the oxygen atom is $1s^2 2s^{1.77} 2p^{5.36}$. Each of the hydrogen atoms has a $1s^{0.39}$ natural occupancy. The NBO charges amount, respectively, to +1.93, −1.14, and +0.61 (×2). These charges, and especially that on the lead atom, are in excellent agreement with those obtained from the NBO analysis using the CRENBS (1.93) and the CRENBLC (1.95) pseudopotentials, and also with the AIM/CRENBLC (1.89), ELF/SDD (1.86), and ELF/CRENBS (1.88) charges. The lone pairs of the oxygen atoms are found to be (i) a $sp^{1.14}$ hybrid pointing from O toward Pb which has the right symmetry to overlap the axial $6p^0$ orbital, and (ii) a pure $2p$ orbital, parallel to another $6p^0$ orbital of $Pb^{2+}$. These conclusions remain the same if using the CRENBS or the CRENBLC pseudopotentials. From this analysis, and especially due to the very small occupation of the $6p$ orbitals, it is clear that the double charge essentially remains on Pb: the charge transfer occurring from the water ligand to the cation is less than 0.1 electron.

The ELF/SDD and ELF/CRENBS decompositions are almost identical: two disynaptic valence basins are observed

and correspond to the OH bonds. The oxygen atom is furthermore given a core basin and two monosynaptic valence basins corresponding to the lone pairs: these two ones are populated by a total of 4.34 electrons. A monosynaptic valence basin (occupation: 2.14) describes the $6s^2$ electrons of the $Pb^{2+}$ cation. The situation is *a priori* different using the small-core CRENBLC pseudopotential. A $C$(Pb) basin now appears and account for 9.93 electrons: these are the $5d^{10}$ external core electrons. Still, $V$(Pb), $C$(O), and two $V$(O,H) basins exist and have the same interpretation and almost the same population as previously. The main difference is the disappearance of the $V$(O) monosynaptic basins: they have evolved into $V$(Pb,O) disynaptic basins, the total population of which amounts to 4.36 electrons. This number is identical to the $V$(O) population found for ELF/SDD and ELF/CRENBLC. In fact, a careful inspection of these basins shows that they are almost identical to the $V$(O) basins observed previously. Only a very weak contribution from the metal is found: it is, however, to be remembered that the metal cation is not expected to provide electrons. The charge transfer obtained from the ELF charges is slightly larger than 0.1 electron, in agreement with the NBO and AIM calculations.

The weakness of this charge transfer lets to think that other reasons are responsible for the stability of the complex: electrostatic effects may be essential. Indeed, the $C_{2v}$ geometry is well explained from orbital and electrostatic notions which, in that case, reinforce each other. It is expected that the stabilization induced by the $Pb^{2+}/H_2O$ charge/dipole interaction is optimal within the $C_{2v}$ symmetry ($\Theta=180°$). Moreover, in such a structure a significant overlap between the axial lone pair of $H_2O$ and an empty $6p$ (axial $6p_z$) orbital of $Pb^{2+}$ can occur, which also favors $\Theta=180°$. Such an overlap also occurs between the $b$ (out-of-plane) lone pair of $H_2O$ and another empty $6p$ orbital of $Pb^{2+}$: this could lead to $\Theta=90°$ but no stabilization from electrostatics is to be expected in that case. In fact, in the 180° conformation, the $b$-symmetry lone pair of $H_2O$ is also parallel to an empty $6p$ orbital of $Pb^{2+}$: an overlap, and, thus, a stabilizing charge transfer from the ligand to the cation is allowed.

The existence of $V$(Pb,O) basins, the attractors of which are localized at only 0.58 Å from the oxygen centers and as far as 2.21 Å from the Pb center, can be seen as another indicator of a dative bond between the cation and the water ligand.[84,85]

The NBO analysis leads to the same conclusion; although not providing bond orbitals between the two fragments, the natural orbitals described below show the proper overlaps ($\sigma$ and $\pi$) to favor a dative bond. From this interpretation it is to be concluded that the binding come from both electrostatic and covalence contributions, the respective contributions of which to the binding energy will be investigated in the next section.

### 2. $[Pb(OH)]^+$

At the B3LYP/SDD level of calculations, for which the molecule is found linear, a NBO analysis shows that Pb(II) is described by the $6s^{1.92}6p^{0.37}$ natural electronic configuration; that of the oxygen atom is $1s^2 2s^{1.81} 2p^{5.48}$. The hydrogen atom has a $1s^{0.41}$ natural occupancy. The NBO charges amount to, respectively, +1.71, −1.29, and +0.59 (Table VIII). In contrast to $[Pb(H_2O)]^{2+}$, a natural bond orbital ensures the Pb–O bond. It corresponds to the overlap of a Pb(II) natural orbital having a 3.6% $6s$ contribution and 96.4% $6p$ (axial) character with an oxygen $sp$ hybrid characterized by a 50.8% $2s$ contribution and 49.2% $2p$ character. The OH bond is ensured by another oxygen $sp$ orbital interacting with $1s_H$. All remaining occupied orbitals exhibit an atomic character.

At the B3LYP/CRENBS and B3LYP/CRENBLC levels, the complex is bent. The NBO analysis does not reveal any important change going from a pseudopotential to the other, and we here report the values obtained for CRENBLC. The natural electronic configuration of Pb(II) is $6s^{1.96}6p^{0.34}$; that of the oxygen atom is $1s^2 2s^{1.84} 2p^{5.41}$. The hydrogen atom has a $1s^{0.44}$ natural occupancy. The NBO charges are, respectively, +1.70, −1.25, and +0.56 (Table VIII). The bonding between the fragments is ensured by a natural orbital built from an almost pure $6p$ orbital for $Pb^{2+}$ and from an $sp$ hybrid for oxygen (10% $s$ character and 90% $p$ character). This orbital is, however, essentially developed on the oxygen atom. The OH bond comes from the interaction of an $sp^{2.2}$ hybrid of the oxygen atom. The lone pairs of the oxygen are, respectively, a pure $2p$ orbital and an in-plane $sp^{0.7}$ hybrid. Still, the remaining occupied orbitals are pure atomic orbitals.

In both cases, the charge transfer from the anionic ligand to the cation is high (about 0.3 electron) and a $\sigma$ covalent bond is formed.

Using the CRENBLC pseudopotential, both ELF and AIM predict an identical charge of 1.56 on the metallic center, which correspond to a 0.44 electron transfer. As seen from Table IX, five ELF basins are obtained. As expected $C$(O) and $V$(O,H) basins appear and integrate to 2.12 and 1.71 electrons, respectively. The $C$(Pb) basin accounts for 9.94 electrons ($5d^{10}$). The $V$(Pb) basin, expected to account for the chemical $6s$ shell, has been enriched by 0.44 electron, essentially coming from oxygen. It is to be noticed that this basin has been repelled from the Pb nucleus with respect to its position in $[Pb(H_2O)]^{2+}$: 1.815 vs 1.733 Å. This is easily explained remembering that

(i) the Pb–O bond length is significantly shorter in $[Pb(OH)]^+$ than in $[Pb(H_2O)]^{2+}$;
(ii) there is a very directional lone pair of the oxygen atom pointing towards $Pb^{2+}$: this is in contrast to the situation observed in $[Pb(H_2O)]^{2+}$, in which the two $V$(O) localization basins exhibit a "rabbit-ear" shape towards $Pb^{2+}$.

Consequently, the electronic density on the Pb nucleus and the attractor as well are shifted outside in order to minimize electronic repulsions. Finally, the $V$(Pb,O) basin is observed and integrates for 5.74 electrons: it accounts for the chemical $2s^2 2p^4$ electrons of the oxygen atom interacting with the metal, 0.30 of them being integrated formally in the $V$(O,H) basin (population amounting to 1.70 electron). The attractor associated with this disynaptic basin is about the same distance from the oxygen center (0.57 Å) but significantly far-

TABLE X. CSOV energy decompositions (kcal/mol) of the B3LYP/PP calculations. *A* stands for the ligand and *B* for Pb(II).

| | $[Pb(H_2O)]^{2+}$ | | | $[Pb(OH)]^{+}$ | | |
|---|---|---|---|---|---|---|
| | CRENBLD $C_{2v}$ | CRENBS $C_{2v}$ | SDD* $C_{2v}$ | CRENBLD $C_s$ | CRENBS $C_s$ | SDD* linear |
| $\Delta E$ | −53.4 | −59.7 | −61.2 | −343.7 | −363.6 | −368.8 |
| $E_1=E_{FC}$ | −21.443 | −25.959 | −17.88 | −238.9 | −242.95 | −226.7 |
| $E_{polB}$ | −1.741 | −1.080 | −2.18 | −16.04 | −16.13 | −22.15 |
| $E_{polA}$ | −15.435 | −15.657 | −16.91 | −37.08 | −45.33 | −43.85 |
| $E_{ctA\rightarrow B}$ | −14.473 | −15.181 | −18.76 | −48.20 | −58.30 | −67.16 |
| $E_{ctB\rightarrow A}$ | −0.188 | −3.155 | −0.99 | −0.353 | −1.70 | −0.72 |
| $E_2$ | −31.837 | −35.073 | −38.84 | −101.67 | −121.46 | −133.88 |
| $\delta E$ | −0.121 | +1.332 | −4.48 | −3.13 | 0.81 | −8.2 |
| E | 40.2% | 43.5% | 29.2% | 69.5% | 66.8% | 61.5% |

ther from the Pb nucleus (2.35 Å) than its analog in $[Pb(H_2O)]^{2+}$. Here, since the three lone pairs remaining on the oxygen center cannot point towards Pb anymore, the attractor corresponding to the 5.74 electron $V(Pb,O)$ basin is not to be found anymore "between" Pb and O, as was the case for the $V(Pb,O)$ attractors in $[Pb(H_2O)]^{2+}$, but it is shifted outside this space, beyond the O center. Although the Pb–O bond length has shortened, the distance between Pb and the attractor associated with the $V(Pb,O)$ basin has thus increased. This valence basin, however, is essentially due to oxygen (for 5.57 electrons): the metal is not expected to provide electron since it is here an acceptor by means of the $6p^0$ orbitals. Such a large transfer (0.43), the existence of a disynaptic valence basin for which the oxygen atom contributes the most, and the fact that the attractor associated with this basin is localized in the vicinity of the oxygen center are in agreement with the NBO analysis and allow concluding for a donor-acceptor interaction between the fragments.

### E. CSOV energy decompositions

From the sole use of the previous analyses, it might be concluded that the stability of these complexes can be explained from a small charge transfer coupled to strong electrostatic interactions. Things may, however, be more subtle and it was found of interest to complement the NBO, AIM, and ELF analyses by interaction energy decompositions. They have been performed within the CSOV scheme as implemented in a modified version of HONDO95.3.[86] The above-defined interaction energy $\Delta E$ between two fragments *A* (ligand) and *B* (metal cation) is split into different components,

$$\Delta E = E_1 + E_2 + \delta E,$$

where

$$E_1 = E_{FC},$$

$$E_2 = E_{pol} + E_{ct} = E_{polA} + E_{polB} + E_{ctA\rightarrow B} + E_{ctB\rightarrow A},$$

$$\delta E = \Delta E - E_1 - E_2.$$

$E_1$ ($E_{FC}$) includes electrostatic and exchange/Pauli repulsion terms.

$E_2$ is the sum of a charge transfer ($E_{ct}$) term and of a polarization ($E_{pol}$) term which both can be split into contributions originating from *A* and *B*.

$\delta E$ accounts for some many-body terms having different physical origins,[87–90] and not considered into the standard CSOV decomposition since they are expected to be small compared to $\Delta E$.

Such an approach has been validated within the framework of DFT[91–95] and has recently been extended to pseudopotential calculations on monohydrate cations of heavy (or not) elements.[55] With such an energy decomposition, it can *a priori* be established clearly what is the dominant origin of the complexation energy; this makes then possible to characterize the complex as a *covalent* ($E_2$ is the largest component in this case) or as an *electrostatic* ($E_1$ is the largest component) species. The weight E of the electrostatic component is defined as

$$\mathsf{E} = E_1/\Delta E.$$

In the version of HONDO we have used, there is no handling of $h(l=5)$ spherical harmonics so that the energy decompositions could not be performed using the exact SDD pseudopotential: we thus use thereafter a modified pseudopotential (SDD*) in which the *h* component has been removed.

#### 1. $[Pb(H_2O)]^{2+}$

It is seen from Table X that this complex results, at the CSOV/B3LYP/CRENBLD and CSOV/B3LYP/CRENBS levels of calculation, from a subtle equilibrium between electrostatic and covalent forces. For CRENBS, $E_1$ amounts to 43.5% (E) whereas $E_2$ accounts for 58.7% of $\Delta E$: there is thus a slight preference for covalence. The analysis of $E_2$ points out to two main contributions. The first one consists in a strong, expected, contribution due to the polarization of water by the dication ($E_{polA}$). This component is reinforced by an equally large contribution originating from the charge transfer occurring from the water ligand toward the dication. This large transfer has by itself two different origins [Fig. 1(d)]. First, the overlap of the two $\sigma$/axial hybrids mentioned

above: such an overlap is recognized by the NBO analysis to be large and stabilizing enough to consider the resulting interaction as bonding. Second, the possible charge transfer from a $p$-$\pi$ lone pair of the water ligand to an empty $p(-\pi)$ orbital of $Pb^{2+}$: the NBO analysis considers that the overlap between these two orbitals is not high enough to characterize it as an effective bond, but the CSOV analysis indicates that such an interaction also significantly contributes to the covalent character of the interaction between the two fragments. These two contributions account for 88% of $E_2$ and for 52% of $\Delta E$. We here recover the interesting conclusion[95] that a small charge transfer as about 0.1 electron can induce important energy stabilization: in the present case, as large as about 15 kcal/mol of the total interaction energy comes from $E_{\mathrm{ct}A\rightarrow B}$. This is about 25% of the total interaction energy. The electrostatic component ($E_1$) accounts for about 42% of the total energy. Moreover, the charge transfer contribution is complemented by an equally large contribution due to the strong polarization of the water ligand: 26% supplemental in favor of $E_2$ are recovered. Just with these two components, covalence overcomes electrostatics. With a E value amounting to about 43.5%, the $[Pb(H_2O)]^{2+}$ entity appears intermediate between the $[Zn(H_2O)]^{2+}$ (43.0%) and $[Cd(H_2O)]^{2+}$ (45.9%) species.[55]

Using SDD* reinforces the value of $E_2$: E falls down to 29.2%, close to the value observed for $[Hg(H_2O)]^{2+}$ (29.5%) in which, as in $[Au(H_2O)]^{+}$ (3.3%), the charge transfer term was found to be the largest component of the interaction energy decomposition due to particular relativistic effects such as the lowering of the $6s^0$ level.[55]

### 2. $[Pb(OH)]^+$

Due to the charged character of both interacting entities, a CSOV analysis (Table X) reveals that $E_1$ is the major stabilizing component of $\Delta E$. The CRENBS charge transfer component from $OH^-$ to $Pb^{2+}$ amounts to −58.30 kcal/mol, a value representing 48% of $E_2$ but only 16% of $\Delta E$. The polarization of the negative charge of the ligand by the doubly charge of the cation is also high: −45.33 kcal/mol. In contrast to the previous complex, these two components altogether cannot overcome the very stabilizing value of $E_1$ resulting from the attraction of an anion by a dication: consequently, the complex is found by the CSOV decomposition to be of electrostatic nature despite the intrinsic high values obtained for the covalent components. The same trends are observed for the SDD* calculations which, as seen previously, slightly reinforces $E_2$ with respect to $E_1$.

Using the B3LYP/CRENBLD approach once again reveals some striking features when compared to B3LYP/CRENBS or to B3LYP/SDD. The 20 kcal/mol difference between both approaches for $\Delta E$ can be explained almost completely by variations in the components of $E_2$ which are equally distributed between the charge transfer from the ligand to the cation and the polarization of the ligand. Both are about 10 kcal/mol lower than at the B3LYP/CRENBS level. These results seem consistent with an improper electronic description of the valence of Pb(II) using the CRENBLD pseudopotential used as such[60] (also see Sec. V).

## VII. CONCLUSIONS

On the basis of comparisons to Hartree-Fock and B3LYP four-component relativistic calculations using an all-electron basis set, the reliability of using scalar relativistic CRENBS or SDD pseudopotentials in describing the $[Pb(H_2O)]^{2+}$ and $[Pb(OH)]^+$ complexes has been established. Close structural and energetical results are obtained when using these pseudopotentials. The results of the population analyses (NBO, AIM, and ELF) are close as well. The CSOV complexation energy decompositions show that both complexes are rather covalent complexes.

$[Pb(H_2O)]^{2+}$ is unambiguously found $C_{2v}$. The ELF/SDD and ELF/CRENBS analyses show two $V$(O) valence basins corresponding to the oxygen lone pairs, whereas the ELF/CRENBL approach exhibits two shared disynaptic $V$(Pb,O) basins. These disynaptic basins reflect the partial covalent character of the interaction found by the CSOV decomposition. They cannot be observed with the large-core SDD and CRENBS pseudopotentials.

$[Pb(OH)]^+$ can be found bent or linear depending on the computational methodology used. When $C_s$ is found, the barrier to inversion through the $C_{\infty v}$ structure is found very low, and could be overcome at high enough temperature, making the molecule floppy, which may have repercussions on its gas-phase rotational and/or vibrational spectra. A dynamic treatment is thus required to get a proper description of this phenomenon and will be reported in due time.

## ACKNOWLEDGMENTS

This research was supported in part by the Intramural Research Program of the National Institute of Health (NIH), and NIEHS. The four-component computations have been supported by IDRIS (F. 91403, Orsay-France) and CINES (F. 34000 Montpellier-France) national supercomputing centers. The authors are indebted to T. Saue (LCQMM-Université Louis Pasteur, Strasbourg, France) for stimulating discussions and a careful reading of the manuscript.

[1] S. J. Lippard and J. M. Berg, *Principles of Bioinorganic Chemistry* (University Science Book, Sausalito, 1994).
[2] S. Hemberg, Am. J. Ind. Med. **38**, 244 (2000).
[3] J. Bressler, K. Kim, T. Chakraborti, and G. Goldstein, Neurochem. Res. **24**, 595 (1999).
[4] H. A. Godwin, Curr. Opin. Chem. Biol. **5**, 223 (2001).
[5] J. J. Chisolm, in *Diagnosis and Treatment of Lead poisoning*, edited by J. J. Chisolm, K. R. Mahaffey, and A. L. Aronson (MSS Information, New York, 1976).
[6] *Le Risque Cancérogène du Plomb: Évaluation en Milieux Professionnels*, directed by B. Hervé-Bazin (EDP Science, Les Ulis, France, 2004).
[7] R. G. Pearson, J. Am. Chem. Soc. **85**, 3533 (1963).
[8] R. G. Pearson, Inorg. Chem. **27**, 734 (1988).
[9] For example, M. Kaupp and P. von Ragué Schleyer, J. Am. Chem. Soc. **115**, 106 (1993).
[10] L. Shimoni-Livny, J. P. Glusker, and C. W. Bock, Inorg. Chem. **37**, 1853 (1998), and references therein.
[11] L. Puskar, P. E. Barran, B. J. Duncombe, D. Chapman, and A. J. Stace, J. Phys. Chem. A **109**, 273 (2005).
[12] T. S. Hofer and B. M. Rode, J. Chem. Phys. **121**, 6406 (2004).
[13] C. Gourlaouen, H. Gérard, and O. Parisel, Chem.-Eur. J. (in press).
[14] C. S. Babu and C. Lim, J. Phys. Chem. A **110**, 691 (2006).
[15] G. Akibo-Betts, P. E. Barran, L. Puskar, B. Duncombe, H. Cox, and A. J. Stace, J. Am. Chem. Soc. **124**, 9257 (2002).
[16] T. Shi, G. Orlova, J. Guo, D. K. Bohme, A. C. Hopkinson, and K. W. M.

Siu, J. Am. Chem. Soc. **126**, 7975 (2004).
[17] A. T. Benjelloun, A. Daoudi, and H. Chermette, J. Chem. Phys. **121**, 7207 (2004).
[18] A. T. Benjelloun, A. Daoudi, and H. Chermette, Mol. Phys. **103**, 317 (2005).
[19] A. T. Benjelloun, A. Daoudi, and H. Chermette, J. Chem. Phys. **122**, 154304 (2005).
[20] X. Wang and L. Andrews, J. Am. Chem. Soc. **125**, 6581 (2003).
[21] X. Wang, L. Andrews, G. V. Chertihin, and P. F. Souter, J. Phys. Chem. A **106**, 6302 (2002).
[22] P. Pyykkö and J. P. Desclaux, Acc. Chem. Res. **12**, 276 (1979).
[23] K. S. Pitzer, Acc. Chem. Res. **12**, 271 (1979).
[24] K. Balasubramanian and K. S. Pitzer, in *Ab Initio Methods in Quantum Chemistry*, edited by K. P. Lawley (Wiley, New York, 1987), Vol. 1.
[25] P. Pyykkö, Chem. Rev. (Washington, D.C.) **88**, 563 (1988).
[26] L. Pisani, J. M. André, M. C. André, and E. Clementi, J. Chem. Educ. **70**, 894 (1993).
[27] *Relativistic Effects in Heavy-Element Chemistry and Physics*, edited by B. A. Heß (Wiley, Chichester, 2003).
[28] A recent state-of-the-art presentation of computational and theoretical relativistic chemistry can be found in the special issue of Chem. Phys. **311**, 1 (2005) dedicated to the memory of Dr. Bernd A. Heß.
[29] N. Kaltsoyannis, J. Chem. Soc. Dalton Trans. **1996**, 1 and references therein.
[30] K. Balasubramanian, J. Chem. Phys. **89**, 5731 (1988).
[31] P. Schwerdtfeger, H. Silberbach, and B. Miehlich, J. Chem. Phys. **90**, 762 (1989).
[32] S. G. Wang and W. H. E. Schwarz, J. Mol. Struct.: THEOCHEM **338**, 347 (1995).
[33] N. A. Richardson, J. C. Rienstra-Kiracofe, and H. F. Schaefer III, J. Am. Chem. Soc. **121**, 10813 (1999).
[34] N. Matsunaga, S. Koseki, and M. S. Gordon, J. Chem. Phys. **104**, 7988 (1996).
[35] H. Cox and A. J. Stace, J. Am. Chem. Soc. **126**, 3939 (2004).
[36] J. Kapp, M. Remko, and P. von Ragué Schleyer, J. Am. Chem. Soc. **118**, 5745 (1996).
[37] A. Szabados and M. Hargittai, J. Phys. Chem. A **107**, 4314 (2003).
[38] S. Escalante, R. Vargas, and A. Vela, J. Phys. Chem. A **103**, 5590 (1999).
[39] S. Varga, B. Fricke, H. Nakamatsu, T. Mukoyama, J. Anton, D. Geschke, A. Heitmann, E. Engel, and T. Basug, J. Chem. Phys. **112**, 3499 (2000).
[40] T. Enevoldsen, L. Visscher, T. Saue, H. J. Aagaard Jensen, and J. Oddershede, J. Chem. Phys. **112**, 3493 (2000).
[41] A. E. Reed, R. B. Weinstock, and F. Weinhold, J. Chem. Phys. **83**, 35 (1985).
[42] A. E. Reed, L. A. Curtiss, and F. Weinhold, Chem. Rev. (Washington, D.C.) **88**, 899 (1988).
[43] E. D. Glendening, A. E. Reed, J. E. Carpenter, and F. Weinhold, NBO, Version 3.1.
[44] R. F. W. Bader, *Atoms in Molecules: A Quantum Theory* (Oxford University Press, Oxford, 2003).
[45] B. Silvi and A. Savin, Nature (London) **371**, 683 (1994).
[46] A. Savin, B. Silvi, and F. Colonna, Can. J. Chem. **74**, 1088 (1996).
[47] A. D. Becke and K. E. Edgecombe, J. Chem. Phys. **92**, 5397 (1990).
[48] A. Savin, R. Nesper, S. Wengert, and T. F. Fässler, Angew. Chem., Int. Ed. **36**, 1808 (1997), and references therein.
[49] For a recent review, see J. Poater, M. Duran, M. Solà, and B. Silvi, Chem. Rev. (Washington, D.C.) **105**, 3911 (2005).
[50] P. S. Bagus, K. Hermann, and C. W. Bauschlicher, Jr., J. Chem. Phys. **80**, 4378 (1984).
[51] P. S. Bagus and F. Illas, J. Chem. Phys. **96**, 8962 (1992).
[52] M. J. Frisch, G. W. Trucks, H. B. Schlegel *et al.*, GAUSSIAN 03, Revision C.02, Gaussian, Inc., Wallingford, CT, 2004.
[53] C. Lee, W. Yang, and R. G. Par, Phys. Rev. B **37**, 785 (1988).
[54] A. D. Becke, J. Chem. Phys. **98**, 5648 (1993).
[55] C. Gourlaouen, J.-P. Piquemal, T. Saue, and O. Parisel, J. Comput. Chem. **27**, 142 (2006).
[56] For a recent review, see, for example, M. Dolg, in *Modern Methods and Algorithms of Quantum Chemistry*, edited by J. Grotendorst (John von Neumann Institute for Computing, Jülich, 2000); or H. Stoll, B. Metz, and M. Dolg, J. Comput. Chem. **23**, 767 (2002).
[57] P. J. Hay and W. R. Wadt, J. Chem. Phys. **82**, 270 (1985).
[58] W. Kuelche, M. Dolg, H. Stoll, and H. Preuss, Mol. Phys. **74**, 1245 (1991).
[59] R. B. Ross, J. M. Powers, T. Atashroo, W. C. Ermler, L. A. LaJohn, and P. A. Christiansen, J. Chem. Phys. **93**, 6654 (1990).
[60] This basis set was obtained from the *Extensible Computational Chemistry Environment Basis Set Database*, Version 02/25/04, as developed and distributed by the Molecular Science Computing Facility, *Environmental and Molecular Sciences Laboratory* which is part of the Pacific Northwest Laboratory, P.O. Box 999, Richland, Washington 99352, and funded by the U.S. Department of Energy. The Pacific Northwest Laboratory is a multiprogram laboraory operated by Battelle Memorial Institute for the U.S. Department of Energy under Contract No. DE-AC06-76RLO 1830; see URL: http://www.emsl.pnl.gov/forms/basisform.html
[61] K. Faegri, Theor. Chem. Acc. **105**, 252 (2001).
[62] Release DIRAC04, 2004; DIRAC, a relativistic ab initio electronic structure program, H. J. Aa. Jensen, T. Saue, L. Visscher *et al.*, see URL: http://dirac.chem.sdu.dk
[63] T. Saue and T. Helgaker, J. Comput. Chem. **23**, 814 (2002).
[64] O. Fossgaard, O. Gropen, M. Corral Valero, and T. Saue, J. Chem. Phys. **118**, 10418 (2003).
[65] L. Visscher and T. Saue, J. Chem. Phys. **113**, 3996 (2000), and references therein.
[66] L. Visscher and K. G. Dyall, At. Data Nucl. Data Tables **67**, 207 (1997).
[67] Original references are to be found in the internal references quoted by GAUSSIAN 03, and may be completed by Ref. 68 and references therein.
[68] V. Barone, J. Chem. Phys. **122**, 14108 (2005).
[69] S. F. Boys and F. Bernardi, Mol. Phys. **19**, 553 (1970).
[70] P. Hobza and R. Zahradnik, Chem. Rev. (Washington, D.C.) **88**, 871 (1988).
[71] T. H. Dunning, J. Chem. Phys. **53**, 2823 (1970).
[72] W. J. Stevens, M. Krauss, H. Bash, and P. G. Jasien, Can. J. Chem. **70**, 612 (1992).
[73] S. Noury, X. Krokidis, F. Fuster, and B. Silvi, TOPMOD package, 1997. This package is available on the website of the Laboratoire de Chimie Théorique, Université Pierre et Marie Curie (UMR CNRS/UPMC 7616), URL: www.lct.jussieu.fr
[74] S. Noury, X. Krokidis, F. Fuster, and B. Silvi, Comput. Chem. (Oxford) **23**, 597 (1999).
[75] A. Pendás, M. A. Blanco, A. Costales, P. Mori Sánchez, and V. Luaña, Phys. Rev. Lett. **83**, 1930 (1999).
[76] O. A. Zhikol, A. F. Oshkalo, O. V. Shishkin, and O. V. Prezhdo, Chem. Phys. **288**, 159 (2003).
[77] A. Sierraalta and F. Ruette, J. Comput. Chem. **15**, 313 (1994).
[78] S. Vyboishchikov, A. Sierraalta, and G. Frenking, J. Comput. Chem. **18**, 416 (1996).
[79] G. Frenking, I. Antes, M. Böhme, S. Dapprich, A. W. Ehlers, V. Jones, A. Neuhaus, M. Otto, and R. Stegmann, in *Reviews in Computational Chemistry*, edited by B. B. Boyd and K. B. Lipkowitz (VCH, New York, 1996), Vol. 8, pp. 63–92.
[80] A. Sierraalta and F. Ruette, Int. J. Quantum Chem. **60**, 1015 (1996).
[81] A. Sierraalta and A. Herize, J. Mol. Struct.: THEOCHEM **529**, 173 (2000).
[82] M. Kohout and A. Savin, J. Comput. Chem. **18**, 2000 (1997).
[83] L. Joubert, B. Silvi, and G. Picard, Theor. Chem. Acc. **104**, 109 (2000).
[84] J. Pilmé, Ph.D. thesis, Université Pierre et Marie Curie (Paris), 2003.
[85] J. Pilmé, M. E. Alikhani, and B. Silvi, J. Phys. Chem. A **109**, 10028 (2005).
[86] M. Dupuis, A. Marquez, and E. R. Davidson, HONDO95.3 Quantum Chemistry Program Exchange (QCPE), Indiana University, Bloomington, IN 47405.
[87] K. Morokuma, J. Chem. Phys. **55**, 1236 (1971).
[88] K. Kitaura and K. Morokuma, Int. J. Quantum Chem. **10**, 325 (1976).
[89] M. S. Gordon and J. H. Jensen, in *Encyclopedia of Computational Chemistry*, edited by P. von Ragué Schleyer (Wiley, Chichester, 1998), Vol. 5, pp. 3198–3214.
[90] W. J. Stevens and W. Fink, Chem. Phys. Lett. **139**, 15 (1987).
[91] M. Neyman, S. Ph. Ruzankin, and N. Rösch, Chem. Phys. Lett. **246**, 546 (1995).
[92] S. C. Chung, S. Kruger, S. Ph. Ruzankin, G. Pacchioni, and N. Rösch, Chem. Phys. Lett. **248**, 109 (1996).
[93] A. M. Márquez, N. López, M. García-Hernández, and F. Illas, Surf. Sci. **442**, 463 (1999).
[94] A. Ricca and C. W. Bauschlicher, J. Phys. Chem. A **106**, 3219 (2002).
[95] J.-P. Piquemal, A. Márquez, O. Parisel, and C. Giessner-Prettre, J. Comput. Chem. **26**, 1052 (2005).